Article

Cobalt(III) Complexes with Thiosemicarbazones as Potential anti-*Mycobacterium tuberculosis* Agents

Carolina G. Oliveira,[a] Pedro Ivo da S. Maia,[b] Marcelo Miyata,[c] Fernando R. Pavan,[c] Clarice Q. F. Leite,[c] Eduardo Tonon de Almeida[d] and Victor M. Deflon,[a]*

[a]*Instituto de Química de São Carlos, Universidade de São Paulo, 13566-590 São Carlos-SP, Brazil*

[b]*Departamento de Química, Universidade Federal do Triângulo Mineiro, 38025-440 Uberaba-MG, Brazil*

[c]*Faculdade de Ciências Farmacêuticas, Universidade Estadual Paulista, 14801-902 Araraquara-SP, Brazil*

[d]*Instituto de Química, Universidade Federal de Alfenas, 37130-000 Alfenas-MG, Brazil*

Complexos de Co^{III} derivados da 2-acetilpiridina N(4)-R tiossemicarbazona (Hatc-R, R = alquil ou aril) foram caracterizados por análise elementar, espectroscopia na região do infravermelho, UV-Visível e ^{1}H RMN, voltametria cíclica (VC), medidas de condutividade e difração de raios X em monocristal. Os resultados obtidos são consistentes com a oxidação do centro de Co^{II} para Co^{III} após a coordenação *N,N,S*-tridentada e monoaniônica dos ligantes tiossemicarbazonas, resultando em complexos octaédricos iônicos do tipo $[Co(atc-R)_2]Cl$. Os estudos de eletroquímica mostram dois processos reversíveis, referentes aos pares redox Co^{III}/Co^{II} e Co^{II}/Co^{I}, que são afetados pelo efeito indutivo dos grupos substituintes na posição N4 dos ligantes. Dois complexos de Co^{III} se mostraram satisfatoriamente ativos, com valores de concentração inibitória mínima abaixo de 10 µmol L^{-1} e um deles apresentou muito baixa citotoxicidade contra células VERO e J774A.1 (IC_{50}), conferindo-lhe altos índices de seletividade (SI > 10).

Co^{III} complexes derived from 2-acetylpyridine N(4)-R thiosemicarbazone (Hatc-R, R = alkyl, aryl) have been characterized by elemental analysis, FTIR, UV-Visible and ^{1}H NMR spectroscopies, cyclic voltammetry (CV), conductimetry measurements and single crystal X-ray diffractometry. The results obtained are consistent with the oxidation of the Co^{II} center to Co^{III} upon coordination of the monoanionic *N,N,S*-tridentate thiosemicarbazone ligands, resulting in octahedral ionic complexes of the type $[Co(atc-R)_2]Cl$. Electrochemistry studies show two reversible processes referring to the redox couples Co^{III}/Co^{II} and Co^{II}/Co^{I} which can be modified by the inductive effects of the substituents groups at the N4 position of the ligands. Two Co^{III} complexes showed satisfactory activity with minimal inhibitory concentration value under 10 µmol L^{-1} and one presented quite low cytotoxicity against VERO and J774A.1 cells (IC_{50}), resulting in high selectivity index (SI > 10).

Keywords: cobalt(III), thiosemicarbazones, anti-*mycobacterium tuberculosis* activity

Introduction

Tuberculosis (TB) still causes the death of millions of people every year, more than any other disease around the world, as described by the World Health Organization (WHO).[1] The pathogenicity of *Mycobacterium tuberculosis* (MTB), the human pathogen responsible for TB, is based on the development of methods to survive inside host cells, comprising the capacity to take possession of macrophages.[2] Despite a 95% efficacious 6-month treatment, the TB problem is still expanding world-wide.[3] It's estimated that one-third of the world's population is infected with dormant forms of MTB, 10% of which will develop the disease among their lives.[4] The actual research on TB has been focused on the increased number of multidrug and extensively drug-resistant TB (MDR- and XDR-TB),[5] especially in HIV-positive patients, giving rise to very high mortality.[6] The number of promising anti-TB drugs following pre-clinical tests has increased and although they involve diverse possible mechanisms, no one targets dormant bacteria, which means that the latent infections cannot be eliminated by the moment.[7] Therefore,

*e-mail: deflon@iqsc.usp.br

it is mandatory to develop new anti-MTB agents that can solve the current therapy problems and inhibit the growth of pathogenic microorganisms in their latent forms.

Biologically active transition metal complexes constitute an increasing research area.[8-11] Metals like Mn, Fe, Co, Ni, Cu and Zn, even in a very low concentration in human body, are responsible for a series essential of biological functions[10] being studied in the bioinorganic chemistry field.[12-14] Cobalt is an essential element for life being the main component of Vitamin B12, which is an essential micronutrient that is required for human health and, more importantly, is required in large quantities by cells that are replicating DNA prior to cell division.[15] Moreover, a lot of new cobalt compounds have been demonstrated to possess particular biological activities, such as antitumor and antibacterial.[16-20]

The interest on the thiosemicarbazones (TSCs) and their metal complexes is due to their versatile chemistry[21] and pharmacological activities,[22-26] which also include anti-TB properties.[11] Frequently, the biological activity presented by the free thiosemicarbazone ligands is enhanced upon complexation.[27] In an effort to select lead candidates for treatment of TB, in the last few years we have studied and reported complexes derived from thiosemicarbazones which presented a high anti-MTB activity.[11] Precisely, V^{IV} and V^{V},[8] Ni^{II}[14] and Mn^{II} complexes[28] derived from 2-acetylpyridine thiosemicarbazones have shown excellent activity against MTB. In this context, we focused our interest in a continuation of the previous studies with some of the first transition metal row by developing now new Co^{III} compounds, cationic instead of neutral complexes as the Ni^{II} and Mn^{II} compounds studied before.[14,28] Hence, believing in the high potential of such compounds as anti-MTB agents and the biochemical features of cobalt, here we describe the preparation of Co^{III} complexes derived from 2-acetylpyridine-thiosemicarbazones, their full characterization as well as the study of their anti-MTB activity and cytotoxicity.

Experimental

Materials

2-Acetylpyridine, thiosemicarbazide, 4-methyl-3-thiosemicarbazide, 4-ethyl-3-thiosemicarbazide, 4-phenyl-3-thiosemicarbazide and analytical reagents grade chemicals and solvents were obtained commercially and used without further purification. 4-Cyclohexyl-3-thiosemicarbazide was prepared as previously described.[27] The ligands Hatc, Hatc-Me, Hatc-Et, Hatc-Ch and Hatc-Ph were prepared by refluxing equimolar ethanolic solutions containing the desired thiosemicarbazide (10 mmol) and 2-acetylpyridine (10 mmol) for 1 h, as reported elsewhere.[29,30]

Instruments

FTIR spectra were measured as KBr pellets on a Shimadzu IR Prestige-21 spectrophotometer between 400 and 4000 cm^{-1}. Elemental analyses were determined using a Leco Instrument, model Truspec CHNS-O. The conductivities of the complexes were measured in 1×10^{-3} mol L^{-1} MeOH or H$_2$O solutions using an Orion Star Series conductometer. UV-visible (UV-Vis) spectra were measured with a Shimadzu UV-1800 spectrophotometer in MeOH solutions. The electrochemical experiments were carried out at room temperature in acetonitrile containing 0.1 mol L^{-1} tetrabutylammonium perchlorate (PTBA) (Fluka Purum) as supporting electrolyte, using an electrochemical analyzer μAutolab III. Cyclic voltammetry experiments were performed with a glassy carbon (CG) working stationary electrode, a platinum auxiliary electrode and an aqueous Ag/AgCl reference, carried out with a rate sweep of 100 mV s^{-1} or 200 mV s^{-1}. The ^{1}H NMR spectra were acquired using equipment Agilent 400/54 Premium Shielded 9.4 T, working at 399.8 MHz for ^{1}H. The NMR spectra were internally referenced to TMS.

Crystal structure determination

Brown crystals of [Co(atc)$_2$]Cl·H$_2$O (**1**·H$_2$O) were grown by slow evaporation of the ethanol mother solution of **1**. Crystals of [Co(atc-Ph)$_2$]·MeOH (**5**·MeOH) were obtained by recrystallization of **5** in MeOH/CH$_2$Cl$_2$ 1:2 at room temperature. The data collections were performed using Mo-Kα radiation (λ = 71.073 pm) on a BRUKER APEX II Duo diffractometer. Standard procedures were applied for data reduction and absorption correction. The structures were solved with SHELXS97 using direct methods,[31] and all non-hydrogen atoms were refined with anisotropic displacement parameters with SHELXL97.[32] The hydrogen atoms were calculated at idealized positions using the riding model option of SHELXL97.[32] Table 1 presents more detailed information about the structures determination.

Determination of MICs

The anti-MTB activity of the compounds was determined as MIC (minimal inhibitory concentration) values by the REMA (Resazurin Microtiter Assay) method according to Palomino *et al.*[33]

Table 1. Crystal data and structure refinement for [Co(atc)$_2$]Cl·H$_2$O (**1**·H$_2$O) and [Co(atc-Ph)$_2$]Cl·MeOH (**5**·MeOH)

	1·H$_2$O	**5**·MeOH
Empirical formula	C$_{16}$H$_{20}$ClCoN$_8$OS$_2$	C$_{29}$H$_{30}$ClCoN$_8$OS$_2$
Formula weight	498.90	665.11
Temperature / K	296(2)	293(2)
Wavelength / Å	0.71073	0.71073
Crystal system	Monoclinic	Monoclinic
Space group	P2$_1$/n	P2$_1$/c
Unit cell dimensions	a = 10.0774(4) / Å α = 90° b = 17.4487(7) / Å β = 91.012(2)° c = 11.6658(4) / Å γ = 90°	a = 9.9167(2) / Å α = 90° b = 23.4163(5) / Å β = 121.17(10)° c = 15.2784(3) / Å γ = 90°
Volume / Å^3	2050.97(14)	3035.55(11)
Z	4	4
Density (calculated) / (mg m^{-3})	1.616	1.455
Absorption coefficient / mm^{-1}	1.197	0.829
F(000)	1024	1376
Crystal size / mm^3	0.19 × 0.17 × 0.06	0.971 × 0.386 × 0.37
Theta range for data collection	2.10 to 25.35°	1.74 to 25.05°
Index ranges	−12 ≤ h ≤ 11, −20 ≤ k ≤ 20, −14 ≤ l ≤ 14	−11 ≤ h ≤ 11, −27 ≤ k ≤ 24, −16 ≤ l ≤ 18
Reflections collected	12598	18887
Independent reflections	[R(int) = 0.0364]	[R(int) = 0.0181]
Completeness to theta = 25.14° / %	99.3	99.2
Absorption correction	Semi-empirical from equivalents	Semi-empirical from equivalents
Max. and min. transmission	0.7452 and 0.6388	0.7452 and 0.6775
Refinement method	Full-matrix least-squares on F^2	Full-matrix least-squares on F^2
Data / restraints / parameters	3725 / 3 / 270	5327 / 0 / 382
Goodness-of-fit on F^2	1.037	1.068
Final R indices [I>2sigma(I)]	R$_1$ = 0.0402, wR$_2$ = 0.0981	R$_1$ = 0.0316, wR$_2$ = 0.0864
R indices (all data)	R$_1$ = 0.0642, wR$_2$ = 0.1112	R$_1$ = 0.0367, wR$_2$ = 0.0895
Largest diff. peak and hole / (e Å^{-3})	1.043 and −0.275	0.290 and −0.220

Cytotoxicity assay

In vitro cytotoxicity assays (IC$_{50}$, half maximal inhibitory concentration) were performed first on VERO epithelial cells (ATCC CCL81). Following this approach, the most selective compound (higher SI) was additionally tested on the J774A.1 (ATCC TIB-67) murine macrophage cell line. Both studies were recorded as reported before in a previously work.[28]

Selectivity index

The selectivity index (SI) was calculated by dividing IC$_{50}$ for VERO cells by the MIC for the pathogen; if SI ≥ 10, the compound is considered suitable for further investigations.[28]

Preparations

The Co^{III} complexes were synthesized by adding 0.25 mmol CoCl$_2$·6H$_2$O to solutions of 0.5 mmol of the desired ligands in EtOH (15 mL). The resulting solutions were stirred for 2 h under reflux. The solutions were kept under slow evaporation at room temperature until brown precipitates were formed. After 3 days the solids were filtered off, washed with hexane and dried under vacuum.

[Co(atc)$_2$]Cl·H$_2$O (**1**·H$_2$O)

Yield 0.085 g (68%). Analysis: Calc. for C$_{16}$H$_{20}$ClCoN$_8$OS$_2$: C, 38.52; H, 4.04; N, 22.46%. Found: C, 39.58; H, 4.19; N, 22.87%. IR (KBr) ν/cm^{-1} 3259, 3101, 1620, 1598, 1035, 773; UV-Vis in 3.2 × 10^{-5} mol L^{-1} MeOH solution [λ / nm (ε / L mol^{-1} cm^{-1})]: 424 (4801), 365 (7289),

309 (14267), 233 (31028); Molar conductivity (Λ_m in H_2O): 106.80 μS cm^{-1}; ^{1}H NMR (DMSO, 399.8 MHz): δ 2.80 (s, 6H, 2CH$_3$C=N), 7.45 (t, 2H, *J* 8.0 Hz, Py-H), 7.86-7.90 (m, 6H, 2Py-H and 2NH$_2$), 8.02 (d, 2H, *J* 8.0 Hz, Py-H), 8.07 (t, 2H, *J* 8.0 Hz, Py-H).

[Co(atc-Me)$_2$]Cl (2)

Yield 0.085 g (67%). Analysis: Calc. for $C_{18}H_{22}ClCoN_8S_2$: C, 42.48; H, 4.36; N, 22.02%. Found: C, 42.68; H, 4.55; N, 21.61%. IR (KBr) ν/cm^{-1} 3190, 1598, 1560, 1076, 773; UV-Vis in 1.96 × 10^{-5} mol L^{-1} MeOH solution [λ / nm (ε / L mol^{-1} cm^{-1})]: 415 (10178), 367 (18214), 314 (24897), 260 (40102); Molar conductivity (Λ_m in H_2O): 160.00 μS cm^{-1}; ^{1}H NMR (DMSO, 399.8 MHz): δ 2.85 (s, 9H, 2CH$_3$C=N and 1CH$_3$NH), 2.97 (s, 3H, CH$_3$NH), 7.45-8.09 (m, 8H, Py-H), 8.16 (s, 1H, NHCH$_3$), 8.80 (s, 1H, NHCH$_3$).

[Co(atc-Et)$_2$]Cl·H$_2$O(3·H$_2$O)

Yield 0.086 g (61%). Analysis: Calc. for $C_{20}H_{28}ClCoN_8OS_2$: C, 43.28; H, 5.09; N, 20.19%. Found: C, 43.83; H, 5.17; N, 20.22%. IR (KBr) ν/cm^{-1} 3197, 1598, 1556, 1078, 773; UV-Vis in 2.98 × 10^{-5} mol L^{-1} MeOH solution [λ / nm (ε / L mol^{-1} cm^{-1})]: 413 (10302), 369 (18993), 315 (25241); Molar conductivity (Λ_m in H_2O): 100 μS cm^{-1}; ^{1}H NMR (DMSO, 399.8 MHz): δ 1.00-1.20 (m, 6H, -CH$_2$CH$_3$), 2.84 (s, 6H, CH$_3$C=N), 3.20-3.43 (m, 4H, -CH$_2$CH$_3$), 7.45-8.08 (m, 8H, Py-H), 8.16 (s, 1H, NHCH$_2$CH$_3$), 8.86 (s, 1H, NHCH$_2$CH$_3$).

[Co(atc-Ch)$_2$]Cl (4)

Yield 0.086 g (53%). Analysis: Calc. for $C_{28}H_{38}ClCoN_8S_2$: C, 52.13; H, 5.94; N, 17.37%. Found: C, 51.71; H, 6.70; N, 16.81%. IR (KBr) ν/cm^{-1} 3201, 1598, 1556, 1072, 775; UV-Vis in 2.48 × 10^{-5} mol L^{-1} MeOH solution [λ / nm (ε / L mol^{-1} cm^{-1})]: 428 (10967), 372 (21129), 316 (25564); Molar conductivity (Λ_m in MeOH): 100 μS cm^{-1}; ^{1}H NMR (DMSO, 399.8 MHz): δ 1.06-1.95 (m, 20H, Ch-H), 2.83 (s, 6H, CH$_3$C=N), 3.84 (s, 2H, CH-Ch), 7.44-8.05 (m, 8H, Py-H), 8.86 (s, 2H, NH-Ch).

[Co(atc-Ph)$_2$]Cl (5)

Yield 0.126 g (80%). Analysis: Calc. for $C_{26}H_{29}ClCoN_8S_2$: C, 53.12; H, 4.14; N, 17.70%. Found: C, 52.80; H, 4.73; N, 17.25%. IR (KBr) ν/cm^{-1} 3174, 1598, 1552, 1074, 752; UV-Vis in 2.21 × 10^{-5} mol L^{-1} MeOH solution [λ / nm (ε / L mol^{-1} cm^{-1})]: 385 (20588), 315 (18190), 253 (37239); Molar conductivity (Λ_m in MeOH): 88 μS cm^{-1}; ^{1}H NMR (DMSO, 399.8 MHz): δ 2.99 (s, 6H, CH$_3$C=N), 7.08 (t, 2H, *J* 6.0 Hz, Ph-H), 7.38 (t, 4H, *J* 8.0 Hz, Ph-H), 7.51 (t, 2H, *J* 6.0 Hz, Py-H), 7.69 (d, 4H, *J* 8.0 Hz, Ph-H), 8.02 (d, 2H, *J* 4.0 Hz, Py-H), 8.12-8.18 (m, 4H, Py-H), 10.37 (s, 2H, NH-Ph).

Results and Discussion

Synthesis of the complexes

Reactions of CoCl$_2$·6H$_2$O with two equivalents of Hatc-R in EtOH under reflux for 2 h results in microcrystalline precipitates of the cobalt complexes **1-5** in good yields (Scheme 1). Elemental analyses are consistent with the formation of cationic complexes [Co(atc-R)$_2$]$^+$, in accordance with the observed molar conductivity values. All the compounds except [Co(atc-Ph)$_2$]Cl are water soluble. They are very soluble in methanol and dimethyl sulfoxide and sparingly soluble in dichloromethane and chloroform, demonstrating a high hydrophilic character.

Infrared, UV-Vis and ^{1}H NMR spectroscopies

The IR spectra of the TSC ligands are characterized by strong broad ν(NH) absorptions in the range 3365-3153 cm^{-1}. One of them, around 3300 cm^{-1}, is absent
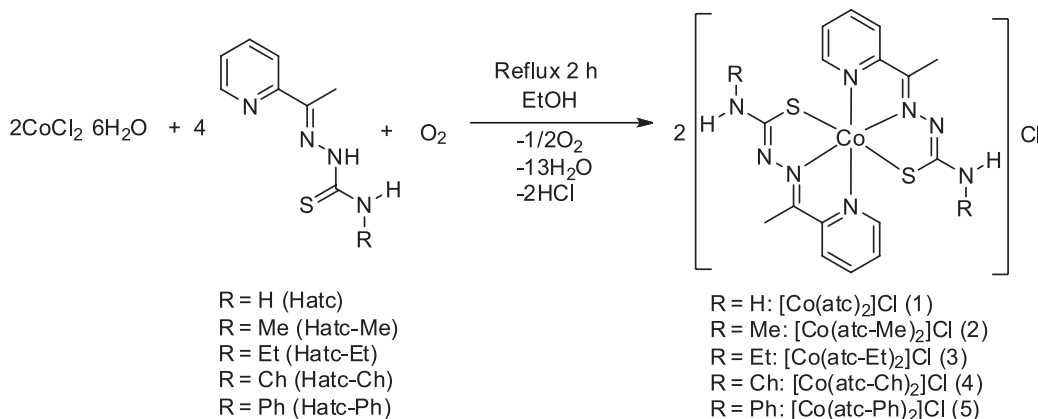
Scheme 1. Synthesis of the Co^{III} complexes.

in the spectra of the Co^{III} cationic complexes, according to the monodeprotonation of these ligands.

The ν(C=N) stretching band found around 1580 cm^{-1} for the free Hatc-R is observed in the 1552-1620 cm^{-1} range for the complexes. The ν(N-N) band at higher frequencies in the IR spectra of the complexes, between 1035 and 1078 cm^{-1}, comparing to those observed for the ligands, in the 989-995 cm^{-1} range, confirms coordination through the azomethine nitrogen atom.[13,34]

The ν(C=S) bands appear in two regions (1118-1074 cm^{-1} and 800-846 cm^{-1}) for the free thiosemicarbazones,[35] while for the complexes the C=S only one band is observed (752-775 cm^{-1}), indicating coordination through the sulfur atom and being consistent with the deprotonation and consequent formation of a C–S single bond in the thiosemicarbazone ligands.[11] The IR absorption bands assigned for the free ligands and their cobalt complexes are consistent with the tridentate coordination of the thiosemicarbazone derivatives in a *N,N,S*-tridentate mode, through the sulfur atom, the azomethine nitrogen and the pyridine nitrogen atoms, forming octahedral complexes.

The electronic spectra of the ligands show a band in the 312-402 nm range, assignable to a combination of internal n$\rightarrow\pi$* and $\pi\rightarrow\pi$*electronic transitions related to the pyridine ring.[30,36-39] The spectra of the Co^{III} complexes show the pyridine ring transitions, with the n$\rightarrow\pi$* occurring at higher energies, below 300 nm, confirming the complexes formation.[40] Additional bands in the 360-400 nm range are assignable as combinations of d$\rightarrow$d transitions with S$\rightarrow$Co^{III} and Py$\rightarrow$Co^{III} charge transfer transitions.[40] Therefore, it was not possible to see the Co^{III} ^{1}T$_{1g}$ $\leftarrow$ ^{1}A$_{1g}$ and ^{1}T$_{2g}$ $\leftarrow$ ^{1}A$_{1g}$ allowed transitions usually observed in the visible region.[41]

The ^{1}H chemical shift values of the free ligands were previously reported.[8,30,35] The Co^{III} complexes show similar ^{1}H NMR behavior, with the hydrogen signals being found as expected. The NH$_2$ hydrogens of complex **1** are found at 7.90 ppm as a broad singlet, while the spectra of the complexes **4** and **5** showed the NH signals at 8.86 and 10.37 ppm, respectively. For the complexes **2** and **3**, however, two different signals relative to NH hydrogen atoms were observed, at 8.81 and 8.16 ppm for **2** and at 8.86 and 8.17 ppm for **3**. This is in accord with the non-equivalence also observed for the methyl and ethyl groups, suggesting that rotation around the C−NHR (R = −CH$_3$, −CH$_2$CH$_3$) bond is not totally restricted.[42] In fact, the methyl groups attached to the NH fragments are also observed at different chemical shifts for **2**, one at 2.97 ppm and another one around 2.85 ppm, overlapped with the signal for the methyl group of the CH$_3$−C=N moiety. The integration for this broad peak (9 H) is consistent with this overlapping. In the case of the complex **3**, however, this observation is difficult to confirm with certainty due to the overlapping of CH$_2$ peak by residual water, while the methyl group appears as a broad multiplet. For the complexes **1**-**5**, the methyl group (CH$_3$−C=N) is observed in the 2.80-2.99 ppm region. The aromatic protons are observed between 7.08 and 8.18 ppm for all the complexes.

Crystal structures

ORTEP drawings of complexes **1**·H$_2$O and **5**·MeOH with numbering scheme are represented in Figure 1. Crystal data and structure refinement for both compounds are depicted in Table 1. The cobalt complexes are monocationic, presenting a chloride as counter ion. The thiosemicarbazone ligands are coordinated to the Co^{III} center in *N,N,S*-tridentate mode
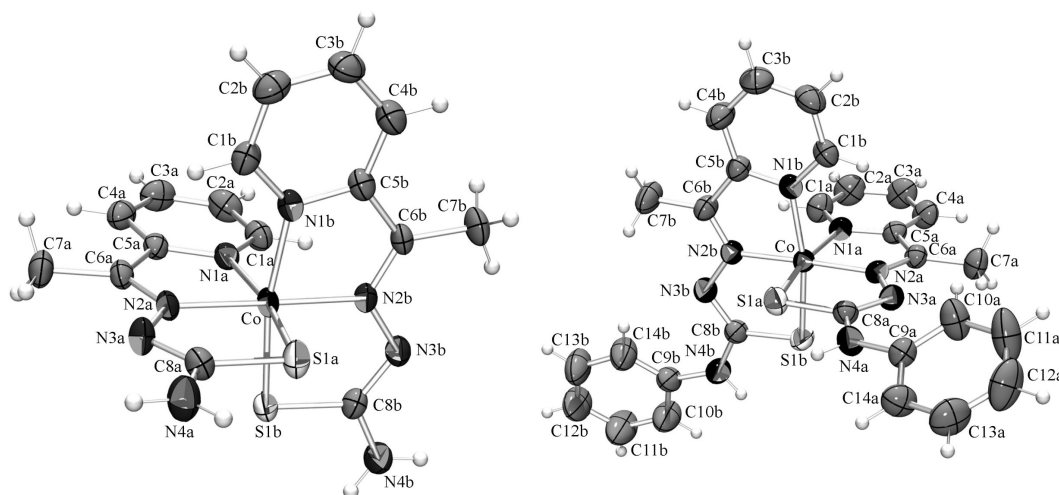
Figure 1. An ORTEP view of [Co(atc)$_2$]Cl·H$_2$O (**1**·H$_2$O) (left) and [Co(atc-Ph)$_2$]Cl·MeOH (**5**·MeOH) (right). Chloride and solvate molecules were omitted for clarity.

and monoanionic form through the pyridine nitrogen atoms N(1A) and N(1B), azomethine atoms N(2A) and N(2B) and sulfur atoms S(1A) and S(1B).

The Co^{III} complexes are clearly characterized by the smaller bond lengths compared to Mn^{II} [Mn(atc-Et)$_2$] compound previously reported.[28] This fact is assigned to the change of the oxidation state +II to +III, resulting in a larger attraction of the electrons from donor atoms of the ligand. This fact is easily observed comparing the distances of Co(1)–N(1) and Mn–N(1) 1.952(3) e 2.2806(15) Å, respectively. The distance Co(1)–S(1A) = 2.2035(6) Å is also shorter compared to Mn–S(1A) = 2.5216(5) Å distance. Furthermore, the bond distances C(8A)–S(1A), 1.745(3) and 1.745(2) Å for complexes **1**·H$_2$O and **5**·MeOH, respectively, are consistent with a single bond character. On the other hand, the bond distance N(3A)–C(8A), 1.321(4) Å in **1**·H$_2$O and 1.314(3) Å in **5**·MeOH, shows a double bond character, in accordance with the deprotonation of the TSCs ligands.

The coordination geometry around the metal center is a distorted octahedron with the tridentate thiosemicarbazone ligands perpendicular to each other with N(1A)–Co(1)–N(2B) being close to 90º in both complexes. A quite smaller distortion of the octahedral angles is observed for the Co^{III} complexes when compared with similar Mn^{II} compounds.[28] This fact can be observed through the bond angle N(2B)–M(1)–N(2A) that is around 159º in [Mn(atc-Et)$_2$] and 178º in the Co^{III} complexes studied here. The bond lengths are similar to those found for other similar Co^{III} complexes.[43] Selected data of interatomic distances and main angles can be found in Table 2.

The crystal structure of **5**·MeOH is stabilized by intermolecular hydrogen bonds, as shown in Figure 2. The nitrogen atom N(4A) is H-bonded through H(4a) to the oxygen atom O(1c) from a methanol molecule, while the nitrogen atom N(4b) is H bonded with a chloride ion Cl(1), which also interacts with a solvate molecule. The interactions build a zigzag alignment of the species parallel to the *c* axis.

The crystal of **1**·H$_2$O is built up by intermolecular hydrogen bonds in diverse directions (see Supplementary Information), which involve the NH$_2$ groups, water solvate molecules and chloride ions.

Electrochemical studies

All complexes presented a similar CV behavior, showed exemplarily for **3** in Figure 3. One irreversible process and two well-defined quasi-reversible ($i_{pa}/i_{pc} \approx 1$) waves are detected. The irreversible peak around 1.2 V is assigned as an oxidation process involving the TSC ligand, as previously reported for a similar compound.[44] The two cathode processes correspond to the Co^{III}/Co^{II} and Co^{II}/Co^{I}

Table 2. Selected bond lengths (Å) and angles (º) refined from X-ray for **1**·H$_2$O and **5**·MeOH

	1·H$_2$O	**5**·MeOH
Bond Lengths		
Co(1)–N(1A)	1.952(3)	1.9579(18)
Co(1)–N(2A)	1.893(2)	1.8861(18)
Co(1)–N(1B)	1.959(3)	1.9659(18)
Co(1)–N(2B)	1.893(2)	1.8826(18)
Co(1)–S(1A)	2.2185(10)	2.2035(6)
Co(1)–S(1B)	2.2151(10)	2.2125(6)
S(1A)–C(8A)	1.745(3)	1.745(2)
S(1B)–C(8B)	1.737(3)	1.741(2)
N(3A)–C(8A)	1.321(4)	1.314(3)
Bond Angles		
N(2A)–Co(1)–N(1A)	82.82(11)	82.73(7)
N(2B)–Co(1)–N(1B)	82.44(11)	82.55(7)
N(2B)–Co(1)–N(1A)	95.85(11)	99.09(8)
N(2B)–Co(1)–N(2A)	178.54(12)	177.90(7)
N(2A)–Co(1)–N(1B)	98.15(11)	98.54(7)
N(1A)–Co(1)–N(1B)	90.23(11)	90.41(7)
N(2B)–Co(1)–S(1A)	95.43(9)	91.96(6)
C(8A)–S(1A)–Co(1)	94.58(12)	94.47(7)
N(1A)–Co(1)–S(1A)	168.72(8)	168.94(6)
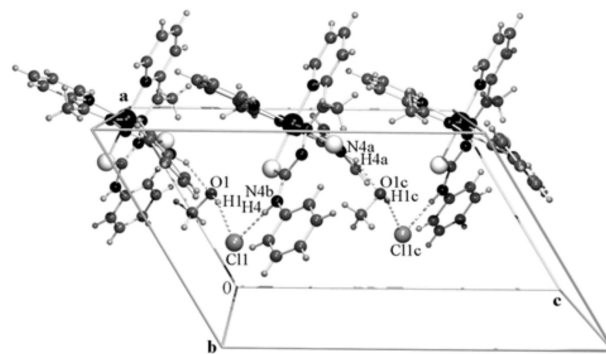
Figure 2. Crystalline and molecular structure of [Co(atc-Ph)$_2$] Cl·MeOH [N(4a)–H(4a)···O(1c) = 158.3º, N(4b)–H(4)···Cl(1) = 177.9º, O(1)–H(1)···Cl(1) = 159.2º]. Symmetry operation used to generate O(1c), H(1c) and Cl(1c): x, −y − 1/2, z − 1/2.

couples, while the two anodic processes correspond to the Co^{I}/Co^{II} and Co^{II}/Co^{III} couples. The complexes presented here have an electrochemical behavior similar to that observed for other Co^{III} complexes already reported.[44]

Through the results depicted in Table 3, it is possible to observe the inductive effects of the R group bonded to the N(4) atom of the thiosemicarbazone ligand on the redox potential values. The electron donating group (R = Ch) tends to provide the more negative potential ($E_{1/2} = -1.10$ V) while the electron withdrawing group
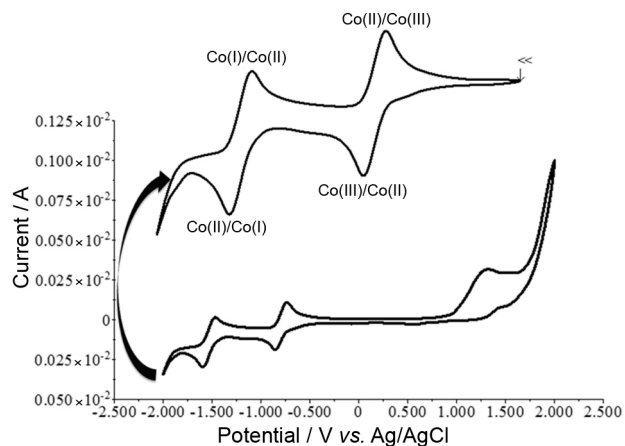
Figure 3. Cyclic voltammogram of [Co(atc-Et)$_2$]$^+$ (scan rate 100 mV s^{-1}) full amplitude and narrow amplitudes.

(R = Ph) shifted the process to a less negative potential (E$_{1/2}$ = −0.70 V), according to the order: −cyclohexyl < −ethyl < −hydrogen < −methyl < −phenyl relative to Co^{III}/Co^{II} couple. In this context, the process relative to the Co^{II}/Co^I couple presents the same trend, demonstrating the same behavior to the first couple. In relation to the second redox pair Co^{II}/Co^I the lower half-wave potential is equal to −1.57 V (complex **4**) and the higher potential is E$_{1/2}$ = −1.46 V (complex **5**). Finally it is evidenced that phenyl stabilizes better the oxidation state +II, while the cyclohexyl group, with electron donating effect, reaches the oxidation state +III easier than the other groups.

We previously reported a similar trend with Mn^{II} complexes relative to oxidation of Mn^{II}/Mn^{III} and Mn^{III}/Mn^{IV} [28] with four of those ligands. However the influence of the groups bonded to N(4) atom observed for Mn^{II} complexes is different for each redox pair. By comparing the values found for manganese complexes, it is possible to conclude that cobalt compounds oxidize much more easily than the manganese ones, since cobalt complexes are stabilized in oxidation state +III.

Biological activity

The biological activity of the compounds was verified by determining the values of MIC against strains of *Mycobacterium tuberculosis* H$_{37}$Rv ATCC 27294. Synthetic compounds with MIC ≤ 12.5 μg mL^{-1} are considered of interest to be further evaluated in cytotoxicity tests, which were primarily evaluated using normal epithelial cells (VERO). Complex **5**, with SI ≥ 10 (SI = IC$_{50}$/MIC) for VERO cells, was further analyzed against macrophages cells J774A.1 (immunologic system cells).

The biological results (anti-MTB activity and cytotoxicity against VERO cells) are shown in Table 4. Two cobalt complexes present MIC ≤ 12.50 μg mL^{-1}, **4** and **5**, with values of 2.41 μmol L^{-1} and 9.87 μmol L^{-1}, respectively. Complex **4** presented a similar activity as the free Hatc-Ch ligand (MIC = 2.82 μmol L^{-1})[27] while complex **5** was more active than the free Hatc-Ph ligand (MIC = 57.75 μmol L^{-1}),[27] in this case improving the activity by complexation. In the other cases the complexation to the Co^{III} didn't lead to improvement on the activities in relation to the free ligands. The cobalt salt CoCl$_2$·6H$_2$O was not effectively active (MIC > 105 μmol L^{-1}) showing that the activity of the complexes cannot be merely associated to the presence of the metal ion. Complex **5** presented quite low cytotoxicity against VERO cells and therefore was also investigated on macrophages cell line J774A.1 (IC$_{50}$ = 988.79 μmol L^{-1}) resulting in high selectivity (SI = 100).

Ni^{II} and Mn^{II} structurally related compounds studied before[14,28] showed to be more active *in vitro* than the Co^{III} analogs studied here. This fact can be explained by the increased polarity of the ionic Co^{III} compounds compared with the neutral Ni^{II} and Mn^{II} complexes, which can influence the permeability through the lipid layer of bacterial membrane resulting in a lower cellular inflow of the active species.[45] Otherwise, the cationic cobalt complexes are very selective and also more water soluble than the neutral nickel or manganese species, which could enhance their absorption *in vivo*, compensating the eventual lower cellular permeation.

The high SI found for complex **5** shows its potential for clinical use, with a wide difference between the concentrations regarding the activity on the pathogen and the cytotoxicity on normal epithelial VERO cells, respectively. Furthermore, at the concentration the complex is active on the pathogen it remains innocuous front the

Table 3. Cyclic voltammetry for the redox couples Co^{III}/Co^{II} and Co^{II}/Co^I for all four complexes, measured in acetonitrile with 0.1 M PTBA as the electrolyte

Complex	E$_{Co^{III}/Co^{II}}$	E$_{Co^{II}/Co^{III}}$	E$_{1/2}$ / V	E$_{Co^{II}/Co^I}$	E$_{Co^I/Co^{II}}$	E$_{1/2}$ /V
1	−0.86	−0.76	−0.80	−1.54	−1.50	−1.52
2	−0.80	−0.73	−0.77	−1.54	−1.47	−1.50
3	−0.86	−0.75	−0.80	−1.60	−1.48	−1.54
4	−1.15	−1.02	−1.10	−1.60	−1.54	−1.57
5	−0.73	−0.65	−0.70	−1.52	−1.41	−1.46

Table 4. Anti-MTB activity (MIC), cytotoxicity (IC_{50}), and selectivity index (SI) of the complexes

Compound	MIC		IC_{50} (VERO cells)		SI^a
	/ μg mL^{-1}	/ μmol L^{-1}	/ μg mL^{-1}	/ μmol L^{-1}	
[Co(atc)$_2$]Cl·H$_2$O (**1**·H$_2$O)	> 25	> 50	434.30	872.05	—
[Co(atc-Me)$_2$]Cl (**2**)	> 25	> 49	483.50	950.69	—
[Co(atc-Et)$_2$]Cl (**3**)	> 25	> 46	95.90	178.89	—
[Co(atc-Ch)$_2$]Cl (**4**)	1.56	2.41	11.80	18.31	7.5
[Co(atc-Ph)$_2$]Cl (**5**)	6.25	9.87	105.30	166.59	17
CoCl$_2$·**6**H$_2$O	> 25	> 105	368.40	3409.2	—
Isoniazid	0.03	0.21	—	—	—

^{a}The selectivity index (SI) was calculated by the ratio IC_{50}^{VERO}/MIC. MIC values for the ligands: Hatc = 31.3 μg mL^{-1} (161.1 μmol L^{-1}); Hatc-Me = 7.8 μg mL^{-1} (37.4 μmol L^{-1}); Hatc-Et = 3.13 μg mL^{-1} (14.08 μmol L^{-1}); Hatc-Ch = 0.78 μg mL^{-1} (2.82 μmol L^{-1}); Hatc-Ph = 15.6 μg mL^{-1} (57.75 μmol L^{-1}).[27]

macrophage cells (J774A.1), which represent the first immune response to the infection.

Conclusions

A series of Co^{III} compounds with thiosemicarbazones ligands, changing the N(4) substituent group by H, methyl, ethyl, cyclohexyl and phenyl could be synthesized in satisfactory yields and fully characterized. The coordination of Hatc-Ph to the Co^{III} was able to enhance the anti-*M. tuberculosis* activity when compared with the free ligand. Moreover the results confirm that structural changes in peripheral group of the ligands can affect significantly the activity against *M. tuberculosis* as well as the cytotoxicity. Complex **5** showed potential biological results, not being the most active on the pathogen, but acting more selectively and thus showing higher potentiality as anti-*M. tuberculosis* agent.

Supplementary Information

Supplementary data are available free of charge at http://jbcs.sbq.org.br as PDF file.

Acknowledgments

References

1. http://www.who.int/tb, accessed in June 2014.

2. Li, R.; Sirawaraporn, R.; Chitnumsub, P.; Sirawaraporn, W.; Wooden, J.; Athappilly, F.; Turley, S.; Hol, W. G. J.; *J. Mol. Biol.* **2000**, *295*, 307.

3. Ananthan, S.; Faaleolea, E. R.; Goldman, R. C.; Hobrath, J. V.; Kwong, C. D.; Laughon, B. E.; Maddry, J. A.; Mehta, A.; Rasmussen, L.; Reynolds, R. C.; Secrist III, J. A.; Shindo, N.; Showe, D. N.; Sosa, M. I.; Suling, W. J.; White, E. L.; *Tuberculosis* **2009**, *89*, 334.

4. Lin, P. L.; Dartois, V.; Johnston, P. J.; Janssen, C.; Via, L.; Goodwin, M. B.; Klein, E.; Barry, C. E.; Flynn, J. L.; *PNAS* **2012**, *109*, 14188.

5. Lun, S.; Guo, H.; Onajole, O. K.; Pieroni, M.; Gunosewoyo, H.; Chen, G.; Tipparaju, S. K.; Ammerman, N. C.; Kozikowski, A. P.; Bishai, W. R.; *Nat. Commun.* **2013**, *4*, 2907.

6. Hong, X.; Hopfinger, A. J.; *Biomacromolecules* **2004**, *5*, 1066.

7. Lång, H.; Quaglio, G.; Olesen, O. F.; *Tuberculosis* **2010**, *90*, 1.

8. Maia, P. I. S.; Pavan, F. R.; Leite, C. Q. F.; Lemos, S. S.; de Sousa, G. F.; Batista, A. A.; Nascimento, O. R.; Ellena, J.; Castellano, E. E.; Niquet, E.; Deflon, V. M.; *Polyhedron* **2009**, *28*, 398.

9. Tarallo, M. B.; Urquiola, C.; Monge, A.; Costa, B. P.; Ribeiro, R. R.; Costa-Filho, A. J.; Mercader, R. C.; Pavan, F. R.; Leite, C. Q. F.; Torre, M. H.; Gambino, D.; *J. Inorg. Biochem.* **2010**, *104*, 1164.

10. Alessio, E.; *Bioinorganic Medicinal Chemistry*, 1st ed.; WILEY-VCH: Trieste, Italy, 2011.

11. Maia, P. I. S.; Graminha, A.; Pavan, F. R.; Leite, C. Q. F.; Batista, A. A.; Back, D. F.; Lang, E. S.; Ellena, J.; Lemos, S. S.; Salistre-de-Araujo, H. S.; Deflon, V. M.; *J. Braz. Chem. Soc.* **2010**, *21*, 1177.

12. Chen, C.; Zhu, X.; Li, M.; Guo, H.; Niu, J.; *Russ. J. Coord. Chem.* **2011**, *37*, 435.

13. Batista, D. da G. J.; Silva, P. B.; Lachter, D. R.; Silva, R. S.; Aucelio, R. Q.; Louro, S. R. W.; Beraldo, H.; Soeiro, M. N. C.; Teixeira, L. R.; *Polyhedron* **2010**, *29*, 2232.

14. Maia, P. I. S.; Pavan, F. R.; Leite, C. Q. F.; Abram, U.; Lang, E. S.; Batista, A. A.; Deflon, V. M. In *Metal Ions in Biology and Medicine and Aqueous Chemistry and Biochemistry of Silicon*. John Libbey Eurotext: Paris, 2011, p. 164–171.

15. Bertini, I.; Gray, H. B.; Lippard, S. J.; Valentine, J. S.; *Bioinorganic Chemistry*, 1st ed.; University Science Books Mill Valley: California, USA, 1994.

16. García-Tojal, J.; García-Orad, A.; Díaz, A. A.; Serra, J. L.; Urtiaga, M. K.; Arriortua, M. I.; Rojo, T.; *J. Inorg. Biochem.* **2001**, *84*, 271.

17. Fan, X.; Dong, J.; Min, R.; Chen, Y.; Yi, X.; Zhou, J.; Zhang, S.; *J. Coord. Chem.* **2013**, *66*, 4268.

18. Ramachandran, E.; Thomas, S. P.; Poornima, P.; Kalaivani, P.; Prabhakaran, R.; Padma, V. V.; Natarajan, K.; *Eur. J. Med. Chem.* **2012**, *50*, 405.

19. Mondelli, M.; Pavan, F. R.; Souza, P. C.; Leite, C. Q. L.; Ellena, J.; Nascimento, O. R.; Facchin, G.; Torre, M. H.; *J. Mol. Struct.* **2013**, *1036*, 180.

20. Hoffman, A. E.; DeStefano, M.; Shoen, C.; Gopinath, K.; Warner, D. F.; Cynamon, M.; Doyle, R. P.; *Eur. J. Med. Chem.* **2013**, *70*, 589.

21. Maia, P. I. S.; Nguyen, H. H.; Hagenbach, A.; Bergemann, S.; Gust, R.; Deflon, V. M.; Abram, U.; *Dalton Trans*. **2013**, *42*, 5111.

22. García-Gallego, S.; Serramía, M. J.; Arnaiz, E.; Díaz, L.; Muñoz-Fernández, M. A.; Gómez-Sal, P.; Ottaviani, M. F.; Gómez, R.; Javier de la Mata, F.; *Eur. J. Inorg. Chem.* **2011**, 1657.

23. Santos, D.; Parajón-Costa, B.; Rossi, M.; Caruso, F.; Benítez, D.; Varela, J.; Cerecetto, H.; González, M.; Gómez, N.; Caputto, M. E.; Moglioni, A. G.; Moltrasio, G. Y.; Finkielsztein, L. M.; Gambino, D.; *J. Inorg. Biochem.* **2012**, *117*, 270.

24. Klayman, D. L.; Bartosevich, J. F.; Griffin, T. S.; Mason, C. J.; Scovill, J. P.; *J. Med. Chem.* **1979**, *22*, 855.

25. Stefani, C.; Punnia-Moorthy, G.; Lovejoy, D. B.; Jansson, P. J.; Kalinowski, D. S.; Sharpe, P. C.; Bernhardt, P. V.; Richardson, D. R.; *J. Med. Chem.* **2011**, *54*, 6936.

26. Soares, M. A.; Lessa, J. A.; Mendes, I. C.; Silva, J. G.; Santos, R. G.; Salum; L. B.; Daghestani, H.; Andricopulo, A. D.; Day, B. W.; Vogt, A.; Pesquero, J. L.; Rocha, W. R.; Beraldo, H.; *Bioorg. Med. Chem.* **2012**, *20*, 3396.

27. Pavan, F. R.; Maia, P. I. S.; Leite, S. R. A.; Deflon, V. M.; Batista, A. A.; Sato, D. N.; Franzblau, S. G.; Leite, C. Q. F.; *Eur. J. Inorg. Chem.* **2010**, *45*, 1898.

28. Oliveira, C. G.; Maia, P. I. S.; Souza, P. C.; Pavan, F. R.; Leite, C. Q. F.; Viana, R. B.; Batista, A. A.; Nascimento, O. R.; Deflon, V. M.; *J. Inorg. Biochem.* **2014**, *132,* 21.

29. Richardson, D. R.; Kalinowski, D. S.; Richardson, V.; Sharpe, P. C.; Lovejoy, D. B.; Islam, M.; Bernhardt, P. V.; *J. Med. Chem.* **2009**, *52*, 1459.

30. West, D. X.; Billeh, I. S.; Jasinski, J. P.; Jasinski, J. M.; Butcher, R. J.; *Transit. Metal Chem.* **1998**, *23*, 209.

31. Sheldrick, G. M.; *SHELXS97*; *Program for the Solution of Crystal Structures*; University of Göttingen, Germany, 1997.

32. Sheldrick, G. M.; *SHELXL97; Program for the Refinement of Crystal Structures*; University of Göttingen, Germany, 1997.

33. Palomino, J. C.; Martin, A.; Camacho, M.; Guerra, H.; Swings, J.; Portaels, F.; *Antimicrob. Agents Chemother.* **2002**, *46*, 2720.

34. Maia, P. I. S.; Nguyen, H. H.; Ponader, D.; Hagenbach, A.; Bergemann, S.; Gust, R.; Deflon, V. M.; Abram, U.; *Inorg. Chem.* **2012**, *51*, 1604.

35. Wiles, D. M.; Gingras, B. A.; Suprunchuk, T.; *Can. J. Chem.* **1967**, *45*, 469.

36. Chan, J.; Thompson, A. L.; Jones, M. W.; Peach, J. M.; *Inorg. Chim. Acta* **2010**, *363*, 1140.

37. Enyedy, E. A.; Primik, M. F.; Kowol, C. R.; Arion, V. B.; Kiss, T.; Keppler, B.; *Dalton Trans*. **2011**, *40*, 5895.

38. West, D. X.; Beraldo, H.; Nassar, A. A.; El-Saied, F. A.; Ayad, M. I.; *Transition Met. Chem.* **1999**, *24*, 595.

39. Pavia, D. L.; Lampman, G. M.; Kriz, G. S.; *Introduction to Spectroscopy. A Guide for Students of Organic Chemistry*; 3rd ed.; Bellingham, USA, 2001.

40. West, D. X.; Lockwood, M. A.; *Transition Met. Chem.* **1997**, *22*, 447.

41. Housecroft, C. E.; Sharpe, A. G. *Inorganic Chemistry*; 2nd ed.; Prentice Hall: Harlow, England, 2005.

42. Nguyen, H. H.; Jegathesh, J. J.; Maia, P. I. S.; Deflon, V. M.; Gust, R.; Bergemann, S.; Abram, U.; *Inorg. Chem.* **2009**, *48*, 9356.

43. Zhu, X. F.; Fan, Y. H.; Wang, Q.; Chen, C. L.; Li, M. X.; Zhao, J. W.; Zhou, J.; *Russ. J. Coord. Chem.* **2012**, *38*, 478.

44. Rodić, M. V.; Leovac, V. M.; Jovanović, L. S.; Vojinović-Ješić, L. S.; Divjaković, V.; Češljević, V. I.; *Polyhedron* **2012**, *46*, 124.

45. Maurya, M. R.; Kumar, A.; Abid, M.; Azam, A.; *Inorg. Chim. Acta* **2006**, *359*, 2439.

Supplementary Information

Cobalt(III) Complexes with Thiosemicarbazones as Potential anti-*Mycobacterium tuberculosis* Agents

Carolina G. Oliveira,[a] Pedro Ivo da S. Maia,[b] Marcelo Miyata,[c] Fernando R. Pavan,[c] Clarice Q. F. Leite,[c] Eduardo Tonon de Almeida[d] and Victor M. Deflon[,a]*

[a]*Instituto de Química de São Carlos, Universidade de São Paulo, 13566-590 São Carlos-SP, Brazil*

[b]*Departamento de Química, Universidade Federal do Triângulo Mineiro, 38025-440 Uberaba-MG, Brazil*

[c]*Faculdade de Ciências Farmacêuticas, Universidade Estadual Paulista, 14801-902 Araraquara-SP, Brazil*

[d]*Instituto de Química, Universidade Federal de Alfenas, 37130-000 Alfenas-MG, Brazil*

Crystallographic data (excluding structure factors) for the structures in this work were deposited in the Cambridge Crystallographic Data Centre as supplementary publication numbers CCDC 988971 (**1**·H$_2$O) and 988972 (**5**·MeOH). Copies of the data can be obtained, free of charge, via www.ccdc.cam.ac.uk/conts/retrieving.html or from the Cambridge Crystallographic Data Centre, CCDC, 12 Union Road, Cambridge CB2 1EZ, UK; fax: +44 1223 336033. E-mail: deposit@ccdc.cam.ac.uk.

IR spectra of compounds
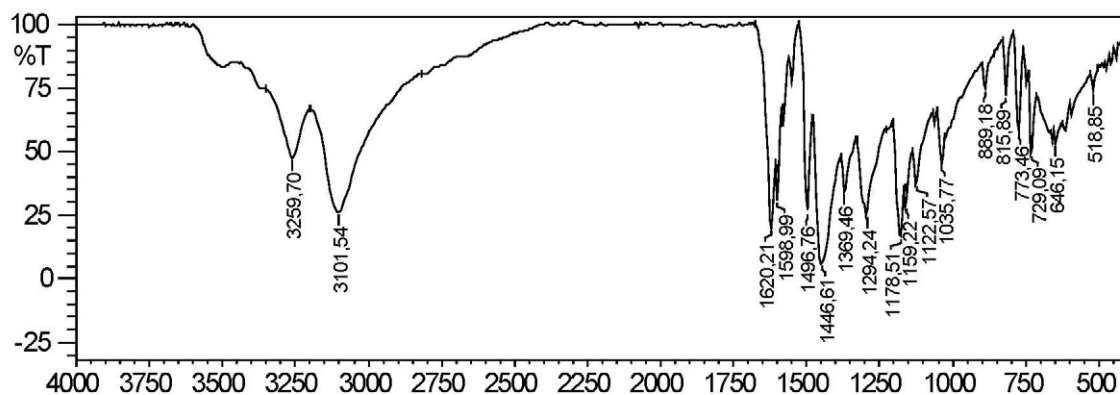
Figure S1. IR spectrum (KBr) of complex **1**.

*e-mail: deflon@iqsc.usp.br
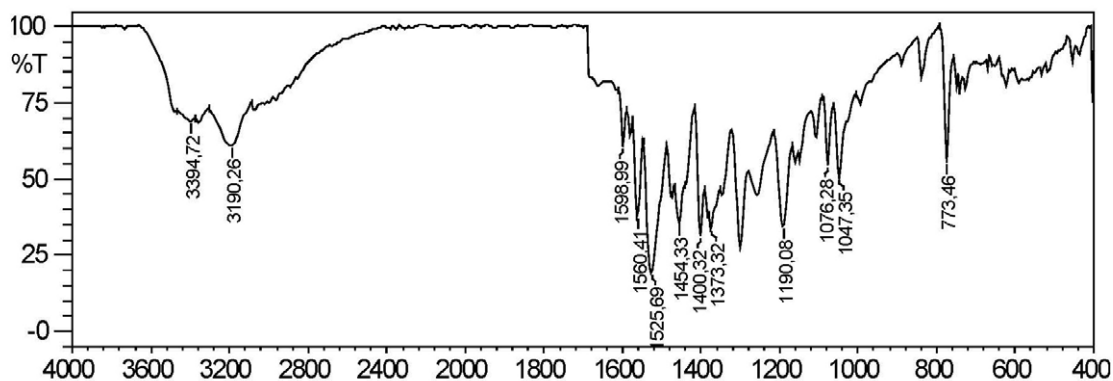
Figure S2. IR spectrum (KBr) of complex **2**.
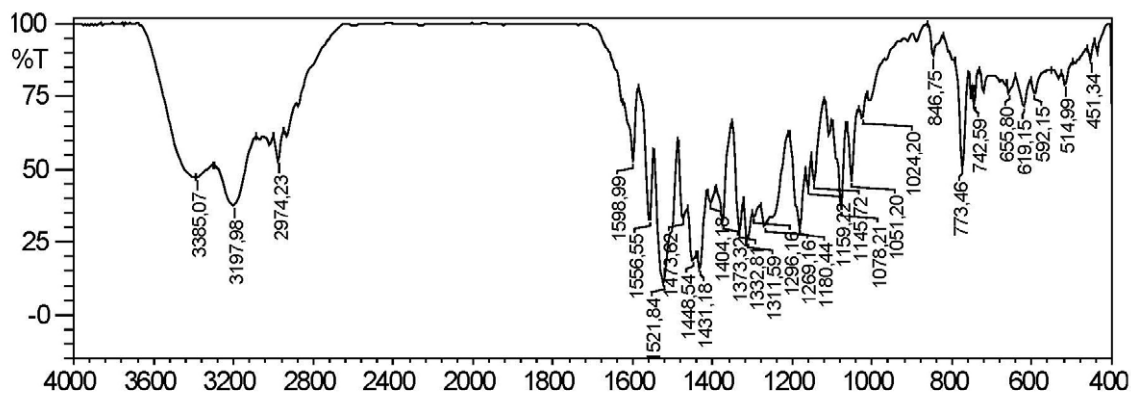
Figure S3. IR spectrum (KBr) of complex **3**.
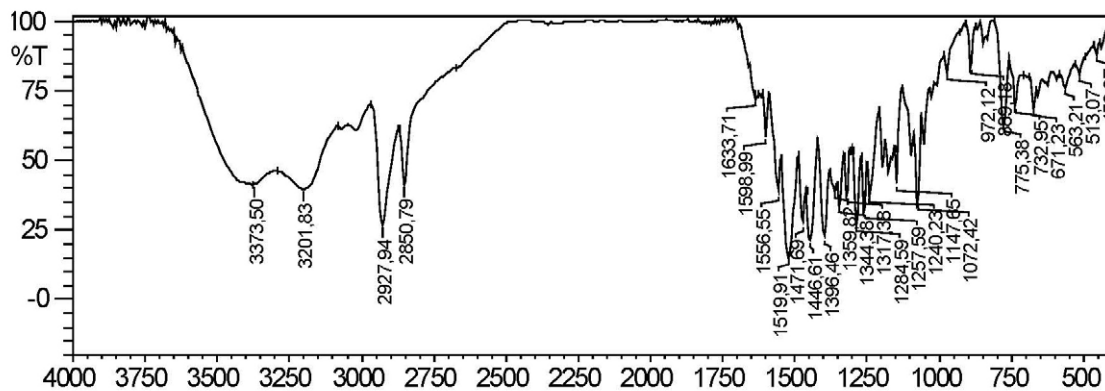
Figure S4. IR spectrum (KBr) of complex **4**.
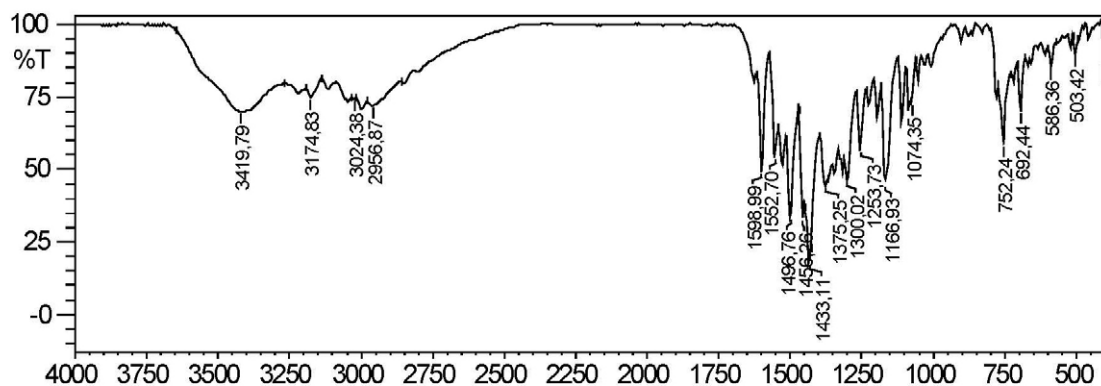
Figure S5. IR spectrum (KBr) of complex **5**.

¹H NMR spectra of compounds
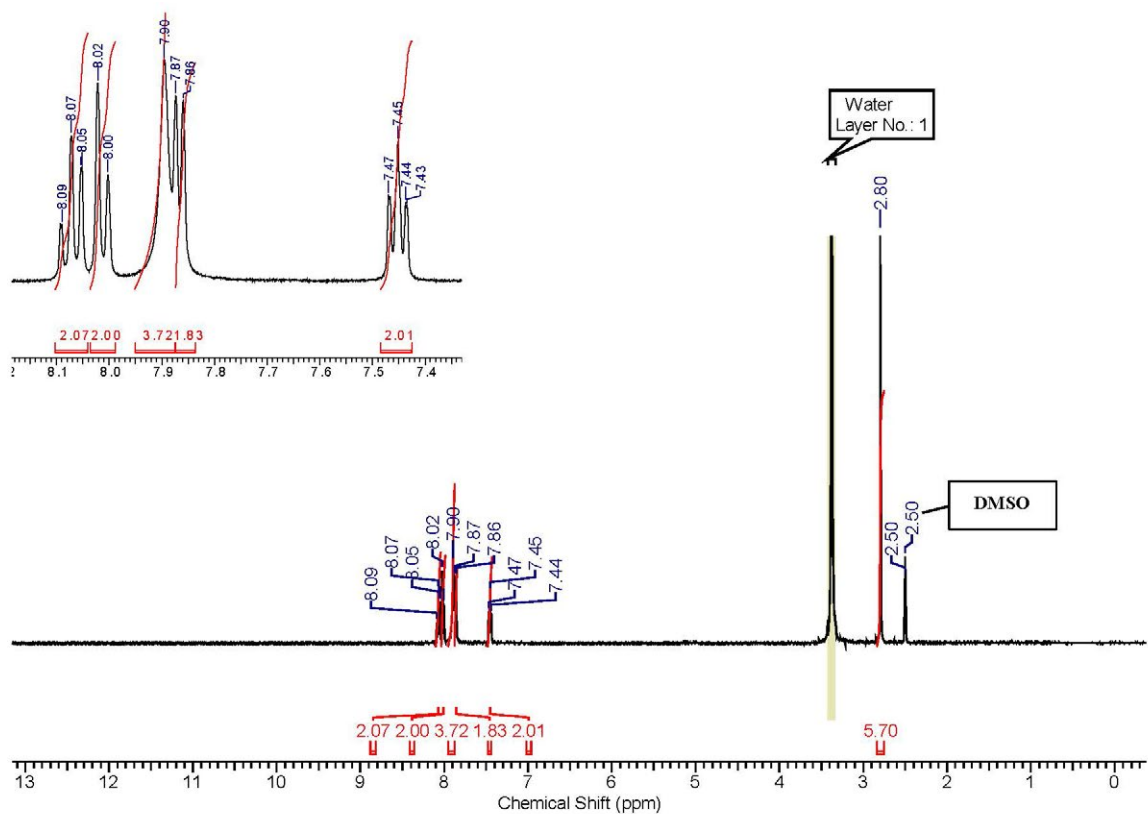
Figure S6. ¹H NMR spectrum (DMSO, 399.8 MHz) of complex **1**.
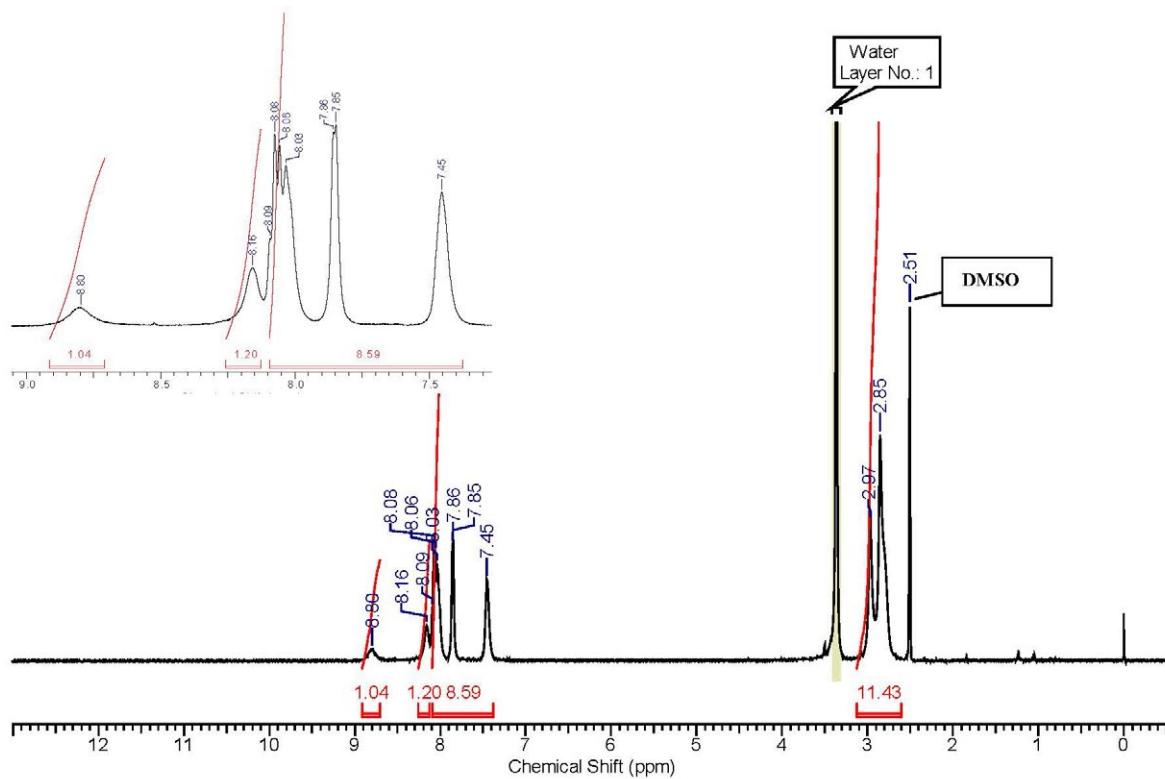
Figure S7. ^{1}H NMR spectrum (DMSO, 399.8 MHz) of complex **2**.
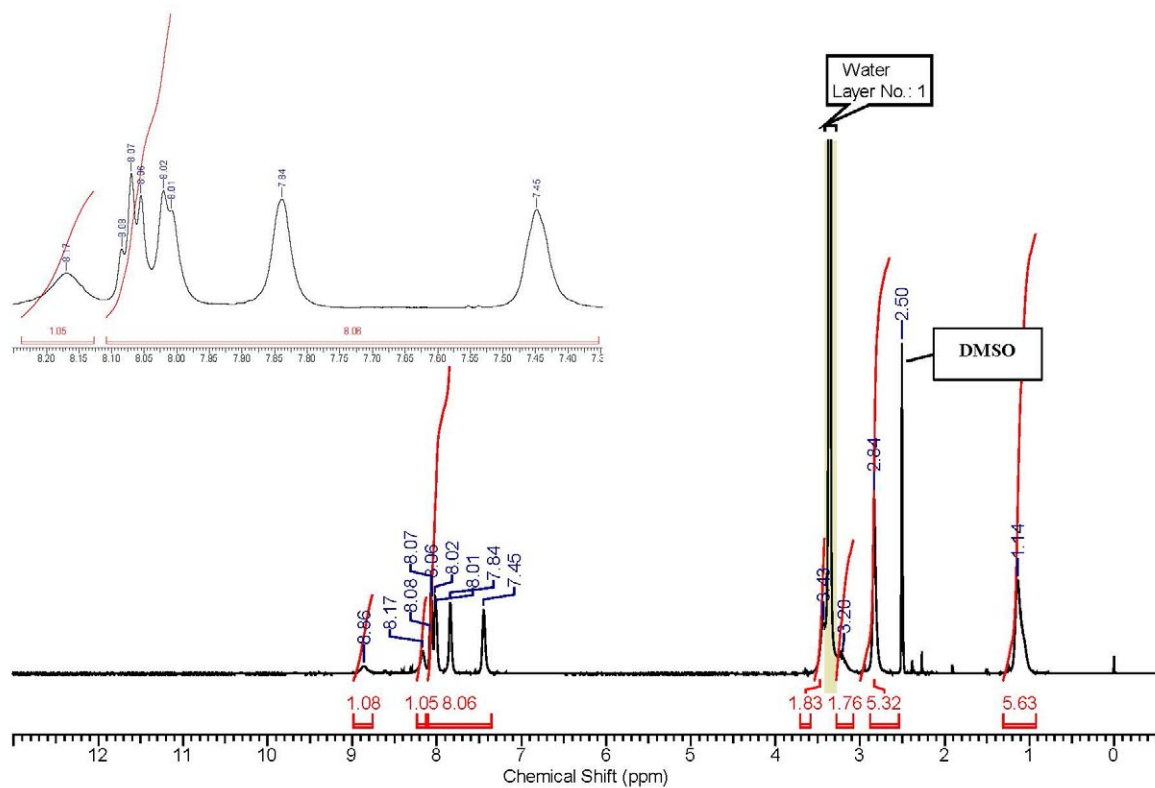
Figure S8. ^{1}H NMR spectrum (DMSO, 399.8 MHz) of complex **3**.
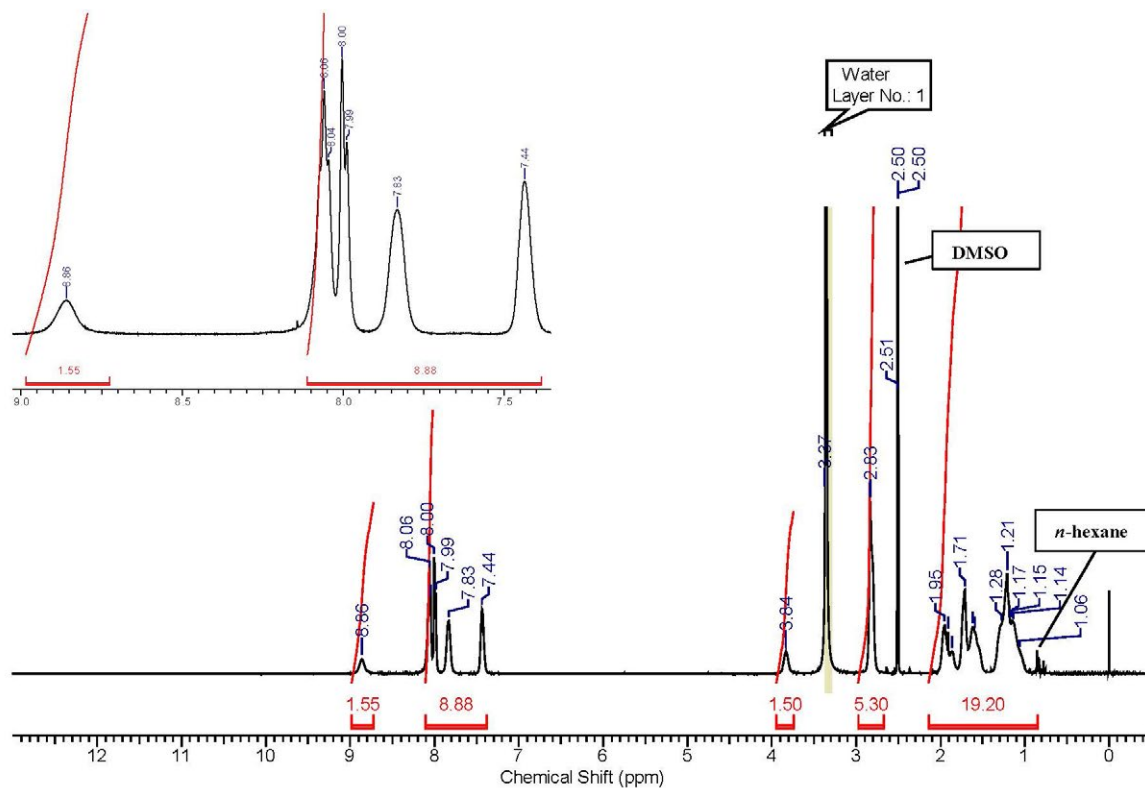
Figure S9. ^{1}H NMR spectrum (DMSO, 399.8 MHz) of complex **4**.
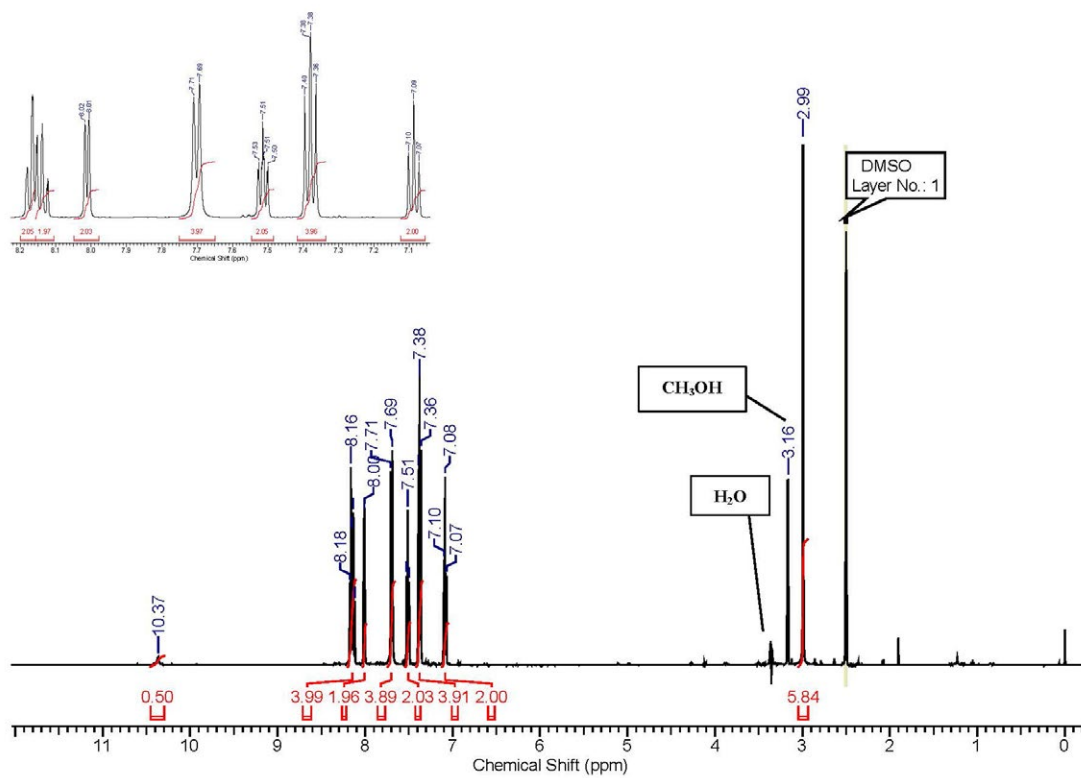
Figure S10. ^{1}H NMR spectrum (DMSO, 399.8 MHz) of complex **5**.
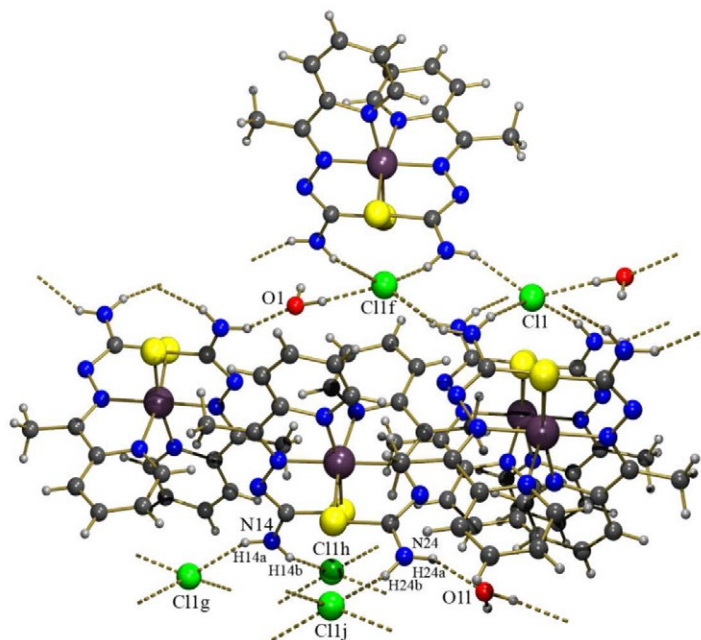
Figure S11. Crystalline and molecular structure of [Co(atc)$_2$]Cl·H$_2$O [N(24)···O(1L) = 2.910(5) Å, N(24)-H(24A)···O(1L) = 146.5°], [N(24)···Cl(1J) = 3.258(3) Å, N(24)-H(24B)···Cl(1J) = 157.6°], [N(14)···Cl(1G) = 3.223(3)Å, N(14)-H(14A)···Cl(1G) = 147.5°], [N(14)···Cl(1H) = 3.222(3)Å, N(14)-H(14B)···Cl(1H) = 152.3°], [O(1)···Cl(1F) = 3.081(4) Å, O(1)-H(1w)···Cl(1F) = 174(4)°]. Symmetry operations used: [F] 1−x,−y, 1−z; [L] 1/2+x,1/2−y,1/2+z ; [J] 1/2+x,1/2−y, −1/2+z; [G] 1/2−x,1/2+y, 1/2−z; [H] −1/2+x,1/2−y, −1/2+z.